PHYSICAL MODELING OF THE MXR PHASE 90 GUITAR EFFECT PEDAL

Conference Paper · September 2014

DOI: 10.13140/2.1.3018.9763

4 authors, including:

Felix Eichas
Helmut Schmidt University
4 PUBLICATIONS **14** CITATIONS
SEE PROFILE

Marco Fink
Ableton
14 PUBLICATIONS **31** CITATIONS
SEE PROFILE

Martin Holters
Helmut Schmidt University
67 PUBLICATIONS **267** CITATIONS
SEE PROFILE

PHYSICAL MODELING OF THE MXR PHASE 90 GUITAR EFFECT PEDAL

Felix Eichas, Marco Fink, Martin Holters, Udo Zölzer

Department of Signal Processing and Communications,
Helmut-Schmidt-Universität
Hamburg, Germany
felix.eichas@hsu-hh.de

ABSTRACT

In this study, a famous boxed effect pedal, also called *stompbox*, for electrical guitars is analyzed and simulated. The nodal DK method is used to create a non-linear state-space system with `Matlab` as a physical model for the *MXR Phase 90* guitar effect pedal. A crucial component of the effect are Junction Field Effect Transistors (JFETs) which are used as variable resistors to dynamically vary the phase-shift characteristic of an allpass-filter cascade. So far, virtual analog modeling in the context of audio has mainly been applied to diode-clippers and vacuum tube circuits. This work shows an efficient way of describing the non-linear behavior of JFETs, which are wide-spread in audio devices. To demonstrate the applicability of the proposed physical model, a real-time VST audio plug-in was implemented.

1. INTRODUCTION

Nodal analysis has been widely used to derive non-linear state-space systems from electrical circuits [1–6]. In this work the version of the nodal DK method described in [1] is applied to the circuit of the *MXR Phase 90* phaser effect. The used modeling technique has the advantage that the state-space matrices can directly be calculated from so called *incidence matrices*, which describe the position of each circuit element in relation to the nodes of the circuit, and *diagonal matrices* which contain the values of the corresponding circuit elements.

The research field of virtual analog modeling in the audio context was so far dominated by studies investigating distortion and overdrive effects. Musical distortion circuits, like diode clippers, and various guitar amplifier and effect circuits are analyzed in [3, 6]. In [4] the main focus lies on modeling of vacuum tubes, which can mainly be found in guitar amplifiers. A dynamic filter broadly used in musical environments, known as Dunlops Crybaby Wah-wah effect pedal, is based on a circuit including two bipolar junction transistors (BJTs). The modeling of the BJTs and the simulation of the effect device was reported in [1]. However, the class of modulation effects was not subject of detailed research so far. Therefore, this paper focuses on modeling a time-variant phasing effect and in particular, the usage of JFETs as non-linear variable resistors in audio circuits.

A slightly modified version of the original circuit by *MXR*, which was available as a D.I.Y. effect pedal kit from [7], is used as the reference device. The circuit of the kit was thoroughly analyzed and every circuit element was measured prior to assembling the pedal. The characteristics of every JFET used in the reference circuit have been measured and are used in the implementation, which is of relevance since they strongly influence the tonal behavior of the effect pedal.

In section 2 a brief review on the nodal DK method, the used discretization method, the handling of operational amplifiers and non-linear elements as well as the used non-linear solver is given. Section 3 describes how the phaser operates in general and discusses the circuit of the analog reference device. In section 4 the results of the measurements are evaluated. Section 5 specifies the real-time VST plug-in implementation, whereas section 6 concludes this paper.

2. NODAL DK METHOD

The nodal DK version of [1] has been used in this work to transfer the effect's schematic to its digital emulation. The laws of Kirchoff, namely Kirchoff's current law (KCL) and Kirchoff's voltage law (KVL), are used to design a state-space system of the circuit under test. The state-space matrices are constructed using *incidence matrices* $\mathbf{N_i}$, which describe the connections of the $\mathbf{i}_{\text{th}}$ group of circuit elements, like resistive, capacitive, or inductive elements, to the nodes of the circuit. A further requirement for constructing the state-space system are *diagonal matrices* $\mathbf{G_i}$, containing the values of the circuit elements and the so called *system matrix*

$$\boldsymbol{S} = \begin{pmatrix} \boldsymbol{N_R^T G_R N_R} + \boldsymbol{N_x^T G_x N_x} & \boldsymbol{N_{vo}} \\ \boldsymbol{N_{vi}} & \mathbf{0} \end{pmatrix} \tag{1}$$

resulting from the afore mentioned incidence and diagonal matrices. $\mathbf{N_i}$ are $m \times n$ matrices with m as the total number of a certain circuit element (e.g. resistors or capacitors) and n as the total number of nodes in the circuit. As it is common for nodal analysis, the reference node (commonly the ground node) is not numbered. The positive and negative poles of every element are marked by a $(+1)$ and a (-1) in each row. If an element is connected to the reference node only the pole of the element which is not connected to the reference node is marked by a (± 1) in the incidence matrix.

The $\mathbf{G_i}$ matrices hold the information about the values of each circuit element and the $\mathbf{N_v}$ matrices give the position of voltage sources in the circuit. Note, that the subindices $\mathbf{R}$ and $\mathbf{X}$ refer to resistive and capacitive elements, respectively.

The procedure uses the trapezoidal discretization rule to get the discrete-time approximations for the energy storing elements of the circuit. In the circuit of the phaser there are only capacitors as energy storing elements. The resulting state-space system has the

form

$$\mathbf{x}(n) = \mathbf{A}\mathbf{x}(n-1) + \mathbf{B}\mathbf{v}(n) + \mathbf{C}\mathbf{i_n}(n) \quad (2)$$

$$\mathbf{y}(n) = \mathbf{D}\mathbf{x}(n-1) + \mathbf{E}\mathbf{v}(n) + \mathbf{F}\mathbf{i_n}(n) \quad (3)$$

$$\mathbf{v_n}(n) = \mathbf{G}\mathbf{x}(n-1) + \mathbf{H}\mathbf{v}(n) + \mathbf{K}\mathbf{i_n}(n). \quad (4)$$

The matrices $\mathbf{A}, \mathbf{B}, \mathbf{C}, \mathbf{D}, \mathbf{E}, \mathbf{F}, \mathbf{G}, \mathbf{H}$, and $\mathbf{K}$ can be computed from $\mathbf{S}, \mathbf{N_i}$, and $\mathbf{G_i}$ (more detailed information on the state-space system is provided in [1]). The actual computation of the state-space system consist of three steps. At first the non-linear relations between the present voltages at the non-linear element $\mathbf{v_n}(n)$ and it's non-linear currents $\mathbf{i_n}(n)$ are obtained through Eq. (4). This is done by an iterative non-linear solver (see section 2.3). Then, the output of the system $y(n)$ can be computed using Eq. (3). At last the internal states $x(n)$ of the system, representing the amount of charge in the capacitors, have to be updated using Eq. (2).

2.1. Capacitors

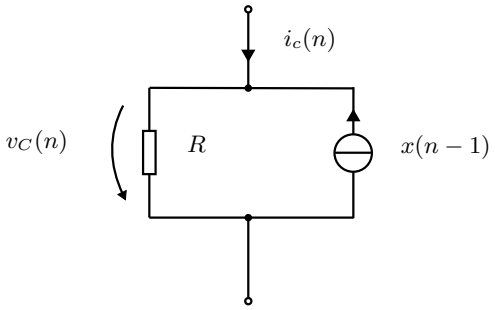

Figure 1: Companion circuit for energy-storing elements of the circuit

From the differential equation, describing the current through a capacitor

$$i_C = C\frac{d\,v_C}{d\,t}, \quad (5)$$

it's discrete-time approximation (using the trapezoidal discretization rule)

$$\frac{1}{2}\left(i_C(n) + i_C(n-1)\right) = \frac{C}{T}\left(v_C(n) - v_C(n-1)\right), \quad (6)$$

and the canonical state

$$x_C(n) = -\frac{2C}{T}v_C(n) - i_C(n) \quad (7)$$

the state-update equation can be formulated

$$x_C(n) = 2\frac{2C}{T}v_C(n) - x_C(n-1). \quad (8)$$

Combining Eq. (7) and Eq. (8) yields

$$i_C(n) = \frac{2C}{T}v_C(n) - x_C(n-1) \quad (9)$$

which describes the companion circuit shown in Fig. 1.
Due to this procedure every capacitor is replaced by a parallel circuit consisting of a resistor $R = \frac{T}{2C}$ and a current source which holds the state information.

2.2. Operational Amplifiers

In this work operational amplifiers are considered to be ideal. They consist of three nodes, describing the inverting input $(-)$, the non-inverting input $(+)$ and the output (out). The ideal operational amplifier (op-amp) is considered as a voltage controlled voltage source, where the voltage difference at the input defines the output voltage $v_{out} = A(v_+ - v_-)$. The input resistance $R_{in} = \infty\,\Omega$ is infinitely large and the output resistance $R_{out} = 0\,\Omega$ infinitely small as illustrated in Fig. 2. A is the open-load amplification factor [5].
Without any op-amp in the circuit the relation between the voltage

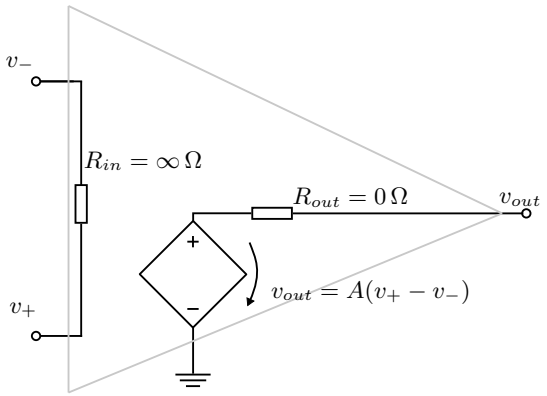

Figure 2: Equivalent circuit diagram for an operational amplifier.

incidence matrices (see section 2) would be

$$\mathbf{N_{vi}} = \mathbf{N_v^T} \quad (10)$$

and

$$\mathbf{N_{vo}} = \mathbf{N_v} \quad (11)$$

with $\mathbf{N_v}$ being of $n \times k$ size. n corresponds to the number of nodes in the circuit while k is the number of voltage sources.
To add an ideal op-amp to the state-space system described in section 2 the only modifications that have to be made are changes in the incidence matrices for the voltage sources $\mathbf{N_v^T}$ and $\mathbf{N_v}$. Therefore, one row is added to the $\mathbf{N_v^T}$ matrix and one column to the $\mathbf{N_v}$ matrix. The additional row in the $\mathbf{N_v^T}$ matrix contains a $(+1)$ at the corresponding node representing the inverting and a (-1) for the non-inverting input of the op-amp respectively

$$\mathbf{r_i} = (\ldots\ 0\ 1\ -1\ 0\ \ldots), \quad (12)$$

which yields

$$\mathbf{N_{vi}} = \begin{pmatrix} N_v^T \\ r_i \end{pmatrix}. \quad (13)$$

This describes the property of an ideal op-amp that it's inputs are at the same potential though they draw no currents.
Since the controlled voltage source describing the op-amps output is connected to the ground node the additional column in the $\mathbf{N_{vo}}$ matrix contains only a $(+1)$ at the corresponding node

$$\mathbf{c_o} = (\ldots\ 0\ 1\ 0\ \ldots)^T \quad (14)$$

leading to

$$\mathbf{N_{vo}} = \begin{pmatrix} \boldsymbol{N_v} & \boldsymbol{c_o} \end{pmatrix}. \quad (15)$$

This describes the voltage source from Fig. 2. By using this technique an ideal op-amp can be easily integrated in the state-space representation and its behavior is described by the peripheral wiring around the op-amp.

2.3. Non-linear Circuit Elements

A major challenge in virtual analog modeling are non-linear elements. Typically, the non-linear relation between voltages and currents are iteratively solved by minimizing an error function $f(x)$ producing the current iteration's residual e. This costly computation has to be performed for every sample and every non-linear component of the desired system. One way to avoid these complex computations, potentially inhibiting real-time functionality, is to pre-compute the non-linear function for a certain range of input values and store the corresponding results in a lookup table. Certainly, the storing of lookup tables requires a decent amount of memory. Hence, an actual implementation is always subject to a compromise between computational complexity and memory requirements.

The non-linear elements in the *Phase 90* circuit are 4 JFETs

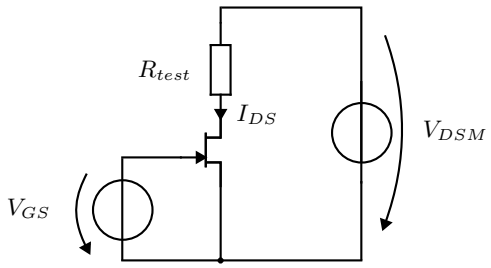

Figure 3: Measurement setup for the JFETs.

which modify the center frequency of the allpass filter cascade and a PNP BJT as a summing amplifier. The input-output characteristic of each JFET was determined by varying the gate-source voltage V_{GS} and drain-source voltage V_{DS} and measuring the drain current I_{DS} of the device. A low-impedance resistor R_{test} was connected in series to the drain-source channel of the JFET for ultrahigh frequency (UHF) stability as can be seen in Fig. 3. The relevant voltage ranges for $V_{DS} \in [-2\,\mathrm{V}, \ldots, 2\,\mathrm{V}]$ and $V_{GS} \in [-2.8\,\mathrm{V}, \ldots, -1.5\,\mathrm{V}]$ were determined using a *SPICE* simulation of the phaser circuit and from measurements on the reference device.

The results of these measurements were saved in lookup tables which are used in the model to calculate the current-voltage relations for every JFET in the circuit.

2.4. Non-linear Solver

As previously mentioned, the non-linear voltage-current relations are solved by iteratively minimizing an error function. The well known Newton-Raphson method has been used to solve the error function

$$f(\mathbf{v_n}(n)) = \mathbf{G}\mathbf{x}(n-1) + \mathbf{H}\mathbf{v}(n) + \mathbf{K}\mathbf{i}(n) - \mathbf{v_n}(n) = e, \quad (16)$$

which is Eq. (4) in a slightly modified form.

The function is linearized at a certain starting value and the root of the linearization is used as the next starting point until the residual of the error function is smaller than a predefined tolerance $f(\mathbf{v_m}) < \epsilon$, as illustrated with listing 1, where m denotes the iteration index and the step size b is 1.

while $|f(\mathbf{v_m})| > \epsilon$ **do**
  $\mathbf{v_{m+1}} = \mathbf{v_m} - b\frac{f(\mathbf{v_m})}{f'(\mathbf{v_m})}$;
end

Algorithm 1: Pseudo code for the Newton-Raphson method.

For the PNP-BJT a damped approach of this method has been implemented. Due to the exponential functions in the Ebers-Moll-Model, describing the BJT, a step with a step size that is too big may lead to a function value which can not be represented by normal floating point arithmetic. Thus the non-linear solver does not converge and this again leads to invalid numbers which can cause the whole state-space system to crash. Therefore the step size of the damped method is halved as long as the resulting residual is bigger than the original residual being computed with the previous step size. Listing 2 shows the corresponding pseudo-code for the implemented method

while $|f(\mathbf{v_m})| > \epsilon$ **do**
  $b = 1$;
  $\mathbf{v_{m+1}} = \mathbf{v_m} - b\frac{f(\mathbf{v_m})}{f'(\mathbf{v_m})}$;
  $\mathbf{v_{\tilde{m}}} = \mathbf{v_{m+1}}$;
  $b = \frac{b}{2}$;
  $\mathbf{v_{\tilde{m}+1}} = \mathbf{v_m} - b\frac{f(\mathbf{v_{\tilde{m}}})}{f'(\mathbf{v_{\tilde{m}}})}$;
  while $|f(\mathbf{v_{\tilde{m}+1}})| > |f(\mathbf{v_{m+1}})|$ **do**
    $b = \frac{b}{2}$;
    $\mathbf{v_{\tilde{m}+1}} = \mathbf{v_m} - b\frac{f(\mathbf{v_{\tilde{m}}})}{f'(\mathbf{v_{\tilde{m}}})}$;
  end
  $\mathbf{v_{m+1}} = \mathbf{v_{\tilde{m}+1}}$;
end

Algorithm 2: Pseudo code for the damped Newton-Raphson method.

3. PHASER EFFECT

Phasing is a common modulation effect in audio applications. Many hardware realizations are based on the following idea. The input signal is sent through an allpass filter cascade which leads to a frequency dependent phase shift. The phase-shifted signal is then added to the original signal which introduces phase cancellation and elevation for certain frequencies. Since each first order allpass filter introduces a maximum phase shift of 180° the amount of resulting spectral notches is half of the number of used allpass stages. The center frequency of each allpass filter is varied by a *low frequency oscillator* (LFO) in the same way. This leads to a time variant phase shift in the output signal of the allpass filter cascade causing the phase cancellation to sway back and forth the frequency axis and thus creating the characteristic effect of the phaser.

3.1. Phase90 Circuit

The circuit of the *Phase90* can be divided into functional blocks, like the power supply block, the low frequency oscillator, and the signal processing blocks which actually process the input signal.

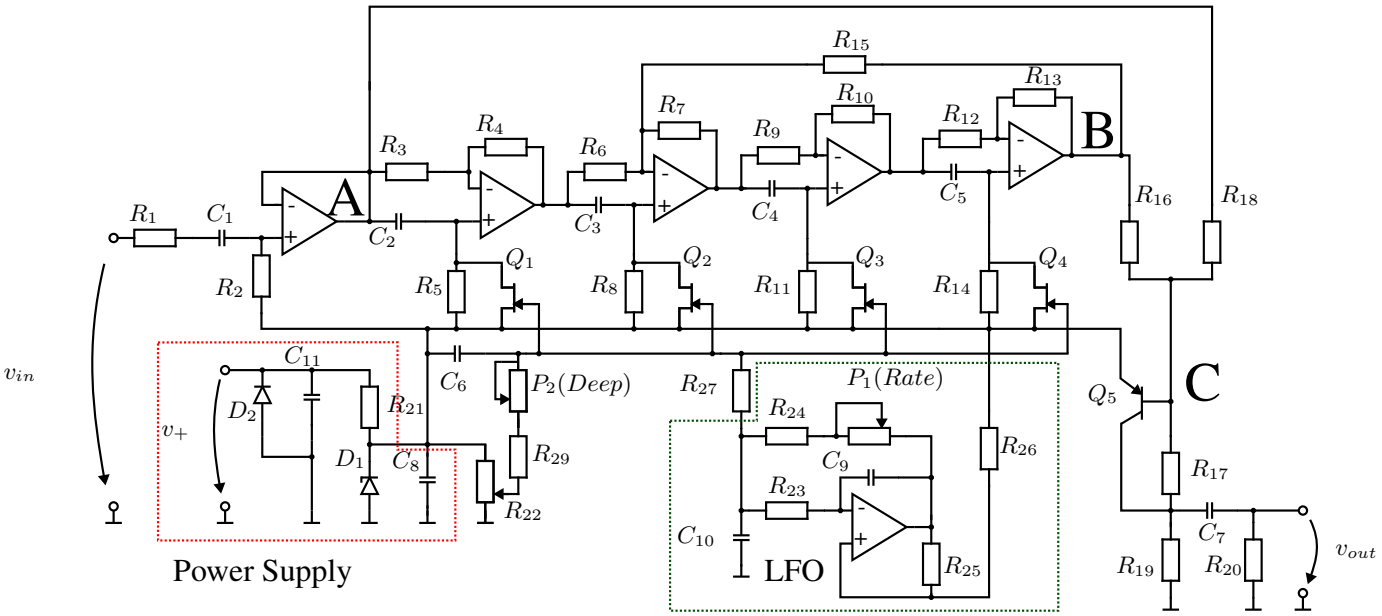

Figure 4: Circuit of the Phase90.

For physical modeling of audio circuits only the signal processing blocks of the device are of interest. Other blocks can be neglected as their contribution would not affect the tonal qualities of the model but increase the computational effort.

In Fig. 4 the negligible blocks of the circuit have been marked as *power supply* and *LFO*. The complete power supply block can be replaced by a voltage source with the value of the voltage defined by the zener diode D_1. This voltage will be called V_{lift} since it adds a constant DC offset of about $V_{\text{lift}} \approx 5\,\text{V}$ to the input signal.

Modeling of the *low frequency oscillator* (LFO) is not necessary since the output of the LFO can be described analytically. The LFO can thus be replaced by another voltage source which produces an oscillating voltage V_{OSC} of the same characteristics as the LFO would create. Due to these simplifications the computational effort of the model is reduced.

The signal path of the circuit contains three main blocks. The first one is the *input stage*, which is just a simple voltage follower, lifting the input signal up to V_{lift}. It consists of an op-amp, R_1, R_2 and C_1. The (A) in Fig. 4 marks the output of the input stage.

Due to their low output resistance, the output of the op-amps are suitable for dividing the blocks of the signal path. After the *input stage* the signal passes a cascade of four allpass filters, using JFETs $Q_1 - Q_4$ as variable resistors. The continuous change of the resistance R_{JFET} leads to alternating center frequencies

$$f_c = \frac{1}{2\pi(R_{fix}||R_{JFET})C_{fix}} \tag{17}$$

of the allpass filters. R_{fix} are the resistors $[R_5, R_8, R_{11}, R_{14}]$, applied in parallel to the JFETs, and C_{fix} denotes the capacitors $C_{2,\ldots,5}$, that are placed at the positive op-amp input. The output of the allpass-stage is marked in Fig. 4 as (B).

The resistance R_{15} introduces a feedback in the allpass cascade which leads to an amplification of certain frequencies. This resonance introduces a harmonic distortion of the amplified frequencies in the output signal of the *Phase 90*. By including a switch or a potentiometer in this feedback path the resonance can be completely switched off or adjusted by the potentiometer allowing a kind of *tone control*. In 1974 the first version of the *Phase 90* was released. The circuit of this early version did not include the feedback path with resistor R_{15}. The so called *script* version (due to it's script font *MXR* logo) is still popular amongst guitar players and reaches horrendous prices in trade. In the state-space model this change of circuitry can be easily adapted leading to a usage of the *Phase 90* model beyond the limitations of the circuit.

The last stage of the signal path is the output stage. The phase-shifted allpass signal is added to the direct signal at the base of the PNP bipolar junction transistor Q_5 driving the output voltage v_{out} of the phaser. Figure 4 illustrates this process: signal (A) is added to signal (B) at the base of the PNP-BJT Q_5 (C).

4. EVALUATION

This section shall present the undertaken experiments, assessing the system's quality. Besides the illustration of the JFET measurements, the static and dynamic behavior of the *Phase 90* emulation is shown in detail. Additionally, the auditory impression is graded.

4.1. JFET Characteristics

The JFETs were measured as described in section 2.3. The results of these measurements can be seen in Fig. 5. The absolute value of the drain-current decreases when the gate-source voltage V_{GS} declines thus increasing the channel resistance of the JFET. In [8] or similar literature the functionality of the JFET is described in detail. To reduce computational complexity the relations between voltages and currents are stored as a lookup table for the efficient calculation of the non-linear element in the circuit.

In this circuit and for the given operating point of the JFETs the

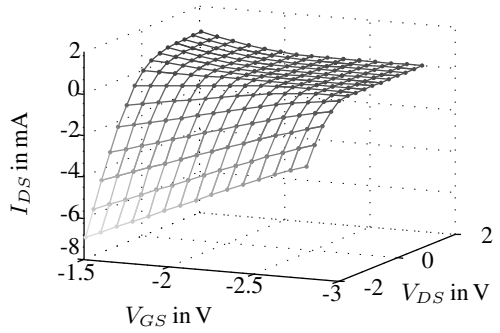

Figure 5: Output characteristic of a single JFET.

gate-source voltage V_{GS} is independent of the drain-source voltage V_{DS} or the drain-current I_{DS}. Since the gate-source voltage is controlled by the LFO it is sufficient to calculate the drain-current drain-source voltage relations subject to the current value of the gate-source voltage which can be computed linearly without the need of a non-linear solver.
Furthermore, it was important to use a matched set of four JFETs with similar characteristics in the reference device. Due to production uncertainties the characteristics of JFETs vary from transistor to transistor. Since all JFETs are driven by the same control voltage an unmatched set of transistors would not have the same operating point and thus the allpass-filters would not be tuned correctly.

4.2. Static Behavior

The connection between resistor R_{27} and R_{24} or capacitor C_{10} respectively was unraveled to disconnect the LFO from the circuit (see Fig. 4) and a voltage source with a constant DC value was applied to this node. A sine wave with the frequency $f_{sin} = 1\,\text{kHz}$ and amplitude of 1 V was fed into the input of the reference device and into the input of the state-space model.

Figure 6 shows the spectra of the output signals for the analog

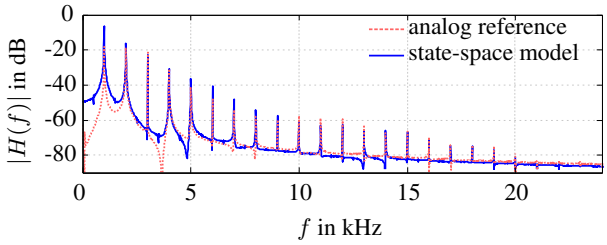

Figure 6: Output spectrum of analog reference device (dashed red line) and state-space model (solid blue line) for a mono-frequent excitation signal with $f_{sin} = 1\,\text{kHz}$ and 1 V amplitude.

reference and the digital model. The model exhibits more signal energy for lower frequencies than the reference device but otherwise the similarity of the distortion behavior of model and system are satisfactory.

4.3. Dynamic Behavior

Since the phaser is a time-variant modulation effect the dynamic behavior is of major importance since it strongly influences the auditory impression. To visualize the varying spectral notches, both

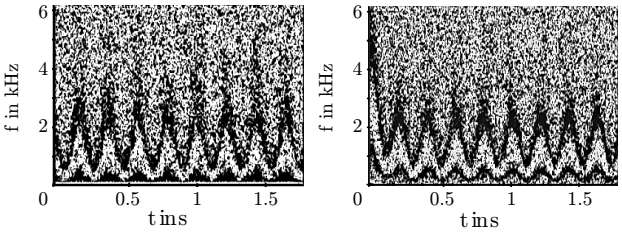

(a) Analog Device (b) State-space model

Figure 7: Output of (a) the analog reference device and (b) the state-space model of the phaser for white noise as the input signal and maximum LFO frequency.

systems were fed with white noise. The output was measured using the maximum depth setting and two settings for the speed: (1) the maximum speed and (2) the minimum speed.
As previously mentioned, the amount of spectral notches is half the number of allpass stages. The Phase90 circuit contains 4 stages and hence, two notches can be seen in Fig. 7 and 8 in form of oscillating dark lines, indicating the frequencies that are canceled.

It is noticeable that the analog signal contains AC hum at

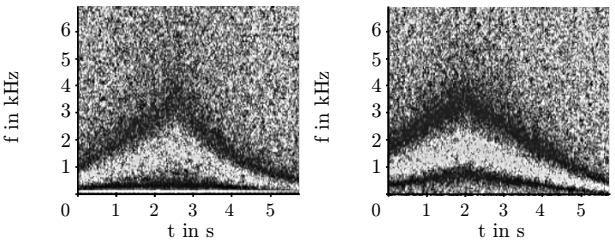

(a) Analog Device (b) State-space model

Figure 8: Output of (a) the analog reference device and (b) the state-space model of the phaser for white noise as the input signal and minimum LFO frequency.

$f = 50\,\text{Hz}$. In Fig. 7.(b) the charging process of the capacitor models can be seen for $t < 0.1\,\text{s}$. When the capacitors are fully charged the frequency cancellation occurs at the same frequencies as in the reference device.
Figure 8 indicates that the approximated output voltage of the state-space LFO does not behave exactly like its analog counterpart. The output voltage of the LFO was approximated by a triangular function while the actual LFO output voltage has slightly curved edges and the falling edge is a little longer than the rising edge.
The notch width of the analog reference device seems larger than for the state-space model while the edges of the notches seem to be sharper in the state-space representation. This is probably caused by noisy side-effects occurring in the JFETs but not in their simplified model.

4.4. Auditory Impression

Despite the afore mentioned differences of state-space model and analog reference device the auditory impression of the model is satisfactory. The difference of the LFO signals is barely noticeable for slower oscillation speeds and perceptually diminishes for faster LFO speeds. Listening examples for the reference device, the emulated system, and the emulated *script* version can be found on line. See [9] for listening examples.

5. REAL-TIME IMPLEMENTATION

State-space implementations are known to be complex due to the necessity to perform many matrix operations. Hence, a real-time implementation was done to test the real-time capability of the phaser emulation. The authors decided to implement a VST plug-in in C/C++ using the well-known JUCE framework [10] that allows straight-forward implementations by simply extending an automatically generated plug-in template with the actual signal processing code.
The circuit was divided in several processing-blocks and the same was done in the real-time implementation. Every module was implemented in a separate class and each object of a module class is a member of the phaser class. There are 6 modules needed to calculate a sample of the output signal. At first the *input* module, then 4 *allpass* modules and at the end of this chain the *output* module. The second *allpass* module is expanded to contain resistance R_{15} and another input to integrate the feedback path mentioned in section 3.1. Alternatively this stage can also be replaced by an *allpass* module without feedback via the graphical user interface of the plug-in to include the afore mentioned 1974 version of the *Phase 90*. The phaser class offers a public processing function, called from the VST host through the JUCE interface, that processes a block of audio data.
Initially the authors planned to use a wide-spread C++ library for linear algebra [11]. It allows a similarly compact representation of matrix operations as `Matlab`. The compact representation, leading to nice readable and maintainable code, is achieved with the help of massive templating. Unfortunately, the implementation based on the templated code was intolerably slow. Hence, a new class providing functionality for memory allocation, addition, multiplication, and copying of matrices was implemented and used from thereon. The computation of the matrices $\mathbf{A}$ to $\mathbf{K}$ of Eq. (2-4) requires the inversion of the potentially large system matrix $\mathbf{S}$. This inversion was performed using the well-known Linear Algebra Package (LAPACK) [12], implemented in Fortran. Using these tools, allows to realize the plug-in, that is now applicable in manifold applications and running real-time. Nevertheless, this first unoptimized, straight-forward implementation utilizes about 70 % of a single Intel i5 processing core.

6. CONCLUSIONS

In this work the circuit of the *MXR Phase 90* was analyzed and emulated using a state-space implementation. A D.I.Y. clone of the effect was assembled and measured to have a reference device. To realize the state-space representation of the effect, the nodal DK method was used, which is a lucid method to transform an analog circuit into a mathematical model. A `Matlab` implementation of the state-space model was developed allowing to imprint the tonal characteristics of the effect on pre-recorded `.wav` files. Additionally a VST plug-in of the effect was implemented in C/C++ to allow real-time application of the *Phase 90*.
The model was analyzed and compared to the reference device in the static (non-oscillating) and the dynamic case. The comparison showed that model and reference are not exactly the same but particularly in the dynamic case the results are very satisfactory. The proposed model also has the possibility to expand the effect beyond the limitations of the circuit. The very first 1974 *script* version of the *Phase 90*, without the resonant feedback, can be used as well as todays version.

7. REFERENCES

[1] M. Holters and U. Zölzer, "Physical modelling of a wah-wah effect pedal as a case study for application of the nodal dk method to circuits with variable parts," in *Proc. Digital Audio Effects (DAFx-11)*, Paris, France, Sept. 19-23, 2011, pp. 31–35.

[2] D. Yeh, J.S. Abel, and J.O. Smith, "Automated physical modeling of nonlinear audio circuits for real-time audio effects. part i: Theoretical development," in *IEEE Trans. Audio, Speech, and Language Process.*, May 2010, vol. 18, pp. 203–206.

[3] D. Yeh, *Digital Implementation of Musical Distortion Circuits by Analysis and Simulation*, Ph.D. thesis, Stanford University, 2009.

[4] K. Dempwolf, *Modellierung analoger Gitarrenverstärker mit digitaler Signalverarbeitung*, Ph.D. thesis, Helmut-Schmidt-Universität, 2012.

[5] J. Macak, *Real-time Digital Simulation of Guitar Amplifiers as Audio Effects*, Ph.D. thesis, Brno University of Technology, 2011.

[6] D. Yeh and J.O. Smith, "Simulating guitar distortion circuits using wave digital and nonlinear state-space formulations," in *Proc. Digital Audio Effects (DAFx-08)*, Espoo, Finland, Sept. 1-4, 2008, pp. 19–26.

[7] Musikding, "Online Material to the Phaser Kit," Website, Available online at `http://diy.musikding.de/?p=384` – accessed February 27th 2014.

[8] U. Tietze and C. Schenk, *Halbleiter Schaltungstechnik*, Springer, Heidelberg, Germany, 1986.

[9] "Listening Examples for the Phase 90," Website, Available online at `http://www2.hsu-hh.de/ant/webbox/audio/eichas/dafx14/audio_examples_local_version.html` – accessed March 17th 2014.

[10] "JUCE Cross-Platform C++," Website, Available online at `http://www.juce.com/` – accessed March 14th 2014.

[11] "C++ linear algebra library," Website, Available online at `http://arma.sourceforge.net/` – accessed March 14th 2014.

[12] "Lapack - linear algebra package," Website, Available online at `http://www.netlib.org/lapack/` – accessed March 14th 2014.